# The Lowest Triplet State of 2-Methylpyrazine

Takeshi WATANABE, Hiroko SHIMADA,† and Ryoichi SHIMADA*

*Department of Chemistry, Faculty of Science, Kyushu University 33, Hakozaki, Higashi-ku, Fukuoka 812*

†*Department of Chemistry, Faculty of Science, Fukuoka University, Nanakuma, Nishi-ku, Fukuoka 814*

(Received February 1, 1982)

The infrared and Raman spectra of 2-methylpyrazine were studied. An assignment was given for all fundamental vibrations based on the polarization behavior of the spectral bands and on the normal coordinate analysis. The magnetic effect on the phosphorescence lifetime and the time-resolved and polarized phosphorescence spectra of this molecule were investigated at 1.4 K. From the analysis of the phosphorescence, (1) the short lifetime phosphorescence was assigned to the emission arising from the most emissive y″ sublevel, as in the case of pyrazine, (2) the long lifetime phosphorescence was assigned to the emissions arising from the x and z″ sublevels, whose lifetimes were roughly equal to each other and (3) the 0-0 and totally symmetric vibronic bands, and the out-of-plane vibronic bands observed in the long lifetime phosphorescence, were ascribed to the z″ and x sublevel emissions, respectively.

The lowest triplet state of pyrazine was assigned to a $^3B_{3u}(n, \pi^*)$ state by Goodman and Kasha[1] and Innes and Gidding.[2] Zalewski, McClure, and Narva[4] pointed out that the lowest triplet state was strongly perturbed by low lying $^3(\pi, \pi^*)$ states through H wagging $\nu_5$ and $\nu_{10a}$ vibrations. Through phosphoresence microwave double resonance (PMDR) and microwave induced delayed phosphorescence (MIDP), a number of workers have discussed the molecular structure of pyrazine in the lowest triplet state and suggested that the molecule, whose equilibrium structure belongs to the point group $D_{2h}$, whould be distorted to $C_{2h}$ or lower symmetry.[4-7]

Lim *et al.*[8] carried out the vibrational analyses of the phosphorescence spectra of pyrazine and its methyl derivatives at 4.2 K and studied the proximity effects on the $T_1 \rightsquigarrow S_0$ radiationless transitions. The enhancement of the radiationless $T_1 \rightsquigarrow S_0$ rate due to methyl substitution was attributed to the distorsion of the potential surface for the $T_1$ state due to the decrease of energy separation between vibronically coupled states.

The study of the phosphorescence process of 3-methylpyrazine should be very interesting because the energy separations between $^3W(n, \pi^*)$ and $^3L_a(\pi, \pi^*)$ states, and $^3W(n, \pi^*)$ and $^3L_b(\pi, \pi^*)$ states are closer than in the case of pyrazine due to methyl substitution. In this paper, an assignment for the normal vibrations of 2-methylpyrazine will be given and then the phosphorescence process, vibronic coupling between $(n, \pi^*)$ and $(\pi, \pi^*)$ states, and distorsion of the molecular structure in the lowest triplet state will be discussed.

## Experimental

*Material.* 2-Methylpyrazine obtained from Aldrich Chemical Company was purified by repeated vacuum distillation followed by zone-refining (about 60 passages). Methylcyclohexane of Dotite Spectrosol grade and *m*-xylene of Merck Reference Substance for gas chromatography were used without further purification. *p*-Dibromobenzene obtained from Wako Chemical Industry was purified by zone-refining (about 60 passages), followed by sublimation under reduced pressure.

*Optical Measurement.* The Raman spectrum was observed in the liquid and solid phases with a JEOL 400T Laser Raman Spectrophotometer. The sample was excited with the 514.5 nm line from an $Ar^+$ ion laser of Toshiba Model LAI-104-A. The depolarization measurement of the individual Raman bands was also made in the liquid.

The infrared spectrum was measured with a Hitachi Infrared Spectrophotometer Model 345 over the range of 4000—250 $cm^{-1}$ in the vapor, liquid, and solid phases. The vapor spectrum was observed at 50 °C with a gas cell 10 cm in optical path. The polarized infrared spectrum was observed in the single crystal with an AgBr wire-grid polarizer by the method described in the previous paper.[9]

The phosphorescence lifetime and spectrum were studied at 1.4 K in methylcyclohexane and *p*-dibromobenzene by the method described in the previous paper.[10] The polarized phosphorescence spectrum of 2-methylpyrazine doped in a *p*-dibromobenzene single crystal was observed at 1.4 K along a, b, and c crystal axes. The single crystal grown in the Bridgman furnace was cut along the cleavage bc plane with a razor. The b and c crystal axes were determined optically with polarized light. Then the crystal was cut along the ac and ab planes. The crystal specimen was held in the dewar so that the normal of the ab or bc plane coincided with the optical axis of the spectrophotometer. The phosphorescence spectra polarized along the a and b axes, or along the b and c axes, were observed. Thus, the relative intensities of individual phosphorescence bands polarized along the a, b, and c axes were obtained.

The magnetic effect of the phosphorescence lifetime of 2-methylpyrazine doped in a *p*-dibromobenzene single crystal was studied at 1.4 K. The sample was set between two poles of a Komatsu Type 100 Electromagnet, which applied a constant magnetic field of 3 K Gauss to the sample. Excitation light from a xenon short arc lamp of Ushio Type UXL-500D was focused on the sample through a Corning glass filter and a solution filter, which acted as a thermal radiation cut filter. The decay of the 0-0 band of the phosphorescence was observed with an oscilloscope by rotating the sample about the crystal axes. The angle between the crystal axis and the magnetic field was calibrated in the following way. After a measurement of the lifetime was over, the xenon lamp was replaced by a miniature lamp. Weak light from the miniature lamp was reflected by the crystal surface in the dewar. The crystal was rotated about the vertical axis, that is, the axis perpendicular to both the magnetic field and the excitation (and phosphorescence) beam, so that the light reflected from the crystal surface went back to the miniature lamp. In this case, the normal of the crystal surface was to coincide with the direction of the excitation beam. The angle of rotation of the crystal directly gave the orientation of

the crystal under measurement.

*Procedure of Normal Coordinate Calculation.* A normal coordinate calculation was performed through the standard GF matirx method with a FACOM M-200 computer at the computer center of Kyushu University. Although the molecular structure of 2-methylpyrazine was not determined yet, it was assumed that the molecular structure belongs to roughly the $C_s$ point group and that the geometric parameters of the ring and the $CH_3$ group were nearly identical with those of pyrazine[11] and toluene,[12] respectively. The F matrix elements for the in-plane and out-of-plane vibrations were evaluated with an improved modification of the Urey-Bradley force field given by Cossee and Schachtschneider[13] and with the valence force field, respectively, as described in the previous paper.[9]

## Results and Discussion

*Normal Vibration.* Force constants for the in-plane and out-of-plane vibrations finally obtained after several iterative calculations are given in Tables 1 and 2, respectively. The internal coordinates for the in-plane and out-of-plane vibrations are illustrated in Fig. 1. The calculated vibrational frequencies and modes are given in Table 3.

The infrared spectrum observed in the single crystal and the Raman spectrum observed in the liquid phase are shown in Figs. 2 and 3, respectively. The polarized infrared spectrum measured with the incident light beams polarized parallel and perpendicular to the direction of the crystal growth of the single crystal will be referred to as // and ⊥ spectra, respectively: these are drawn with solid and dotted lines, respectively.

The polarized infrared bands observed in the single crystal could be classified into two types according to their polarization character. The bands belonging to the first type appear strongly in the // spectrum and weakly in the ⊥ spectrum, while the second type bands appear strongly in the ⊥ spectrum and weakly in the // spectrum. These two types of the bands will be referred to as types A and B, respectively.

Table 1. In-plane force constants

| | | | |
|---|---|---|---|
| $K_{N-C}=K_{N-C'}$ | 5.60 | $F_{C\cdots C''}$ | 0.65 |
| $K_{C-C'}=K_{C-C}$ | 4.45 | $F_{C\cdots H}=F_{C'\cdots H'}$ | 0.50 |
| $K_{C'-C''}$ | 3.20 | $F_{N\cdots H}=F_{N\cdots H'}$ | 0.41 |
| $K_{C-H}=K_{C-H'}$ | 4.50 | $\rho$ | 0.32 |
| $K_{C''-H''}$ | 4.56 | $k^o_{r,r}$ | 0.07 |
| $H_{C-N-C}$ | 0.30 | $k^o_{r,r''}$ | 0.30 |
| $H_{C'-N-C}$ | 0.30 | $k^o_{r'',r''}$ | 0.20 |
| $H_{N-C'-C}$ | 0.48 | $k^m_{r,r}$ | 0.06 |
| $H_{N-C-C}=H_{N-C-C'}$ | 0.45 | $h^m_{R,\alpha}$ | −0.10 |
| $H_{N-C'-C''}=H_{C-C'-C''}$ | 0.15 | $h^m_{R,\alpha'}$ | −0.02 |
| $H_{C-C-H}=H_{C'-C-H}$ | 0.25 | $h^m_{R,\beta}=h^m_{R,\beta'}$ | 0.03 |
| $H_{N-C-H}$ | 0.24 | $f^o_{\alpha,\alpha}=f^o_{\alpha,\alpha'}$ | 0.06 |
| $H_\mu$ | 0.45 | $f^o_{\beta,\beta}=f^o_{\beta,\beta'}$ | 0.10 |
| $H_\nu$ | 0.53 | $f^o_{\mu,\mu}$ | 0.005 |
| $F_{C\cdots C}=F_{C\cdots C'}$ | 0.90 | $f^o_{\nu,\nu}$ | −0.04 |
| $F_{N\cdots C}=F_{N\cdots C'}$ | 0.70 | $f_{\tau,\mu}$ | 0.30 |
| $F_{N\cdots C}$ | 0.90 | $f_{\tau,\nu}$ | 0.35 |

Force constants denoted by $K$, $H$, $F$, and $k$ are given in J/dm²(=mdyn/Å) units, and those denoted by $h$ and $f$ are in pJ/dm·rad(=mdyn/rad) and aJ/rad² (=mdynÅ/rad²) units, respectively.

Table 2. Out-of-plane force constants

| | |
|---|---|
| $Q_{C-N}=Q_{C'-N}$ | 0.20 aJ/rad² |
| $Q_{C-C}=Q_{C'-C}$ | 0.22 |
| $Q_{C'-C''}$ | 0.077 |
| $P_H$ | 0.31 |
| $P_{H'}$ | 0.24 |
| $P_{C''}$ | 0.22 |
| $q^o_{\tau,\tau}$ | −0.06 |
| $q^o_{\tau,\tau'}$ | −0.01 |
| $q^m_{\tau,\tau}$ | −0.008 |
| $p^o_{H,H}$ | 0.075 |
| $p^o_{H',C''}$ | 0.055 |
| $p^m_{H,H'}=p^m_{C'',H}$ | −0.055 |
| $t^o_{\tau,H}=t^o_{\tau,H'}$ | −0.02 |
| $t^m_{\tau,H}=t^m_{\tau,H'}=t^m_{\tau',H'}$ | −0.02 |
| $t^m_{\tau,C''}$ | −0.005 |
| $f^o_{\tau',\mu}$ | 0.30 |
| $f^o_{\tau',\nu}$ | 0.35 |

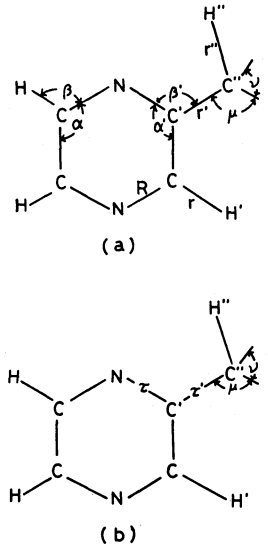


Fig. 1. Internal coordinates for the in-plane (a) and out-of-plane (b) vibrations.

Calculation of the principal moments of inertia indicates that the c axis of the moment is perpendicular to the molecular plane, the a axis is directed nearly along the C–$CH_3$ bond, and the b axis is perpendicular to both a and c axes. These axes will be referred to as the molecular axes. Careful observation of the rotational band envelopes of the infrared bands observed in the vapor phase showed that the bands could be classified into three types: A, B, and C, according to Ueda and Shimanouchi.[14]

*In-plane Vibration*: Bands observed at 342, 1031, and 1065 $cm^{-1}$ in the infrared vapor spectrum showed a typical B band envelope and the corresponding bands in the single crystal showed type B character. Bands observed at 631, 1255, 1308, and 1408 $cm^{-1}$ in the vapor showed a typical A band envelope and the corresponding single crystal bands showed type A

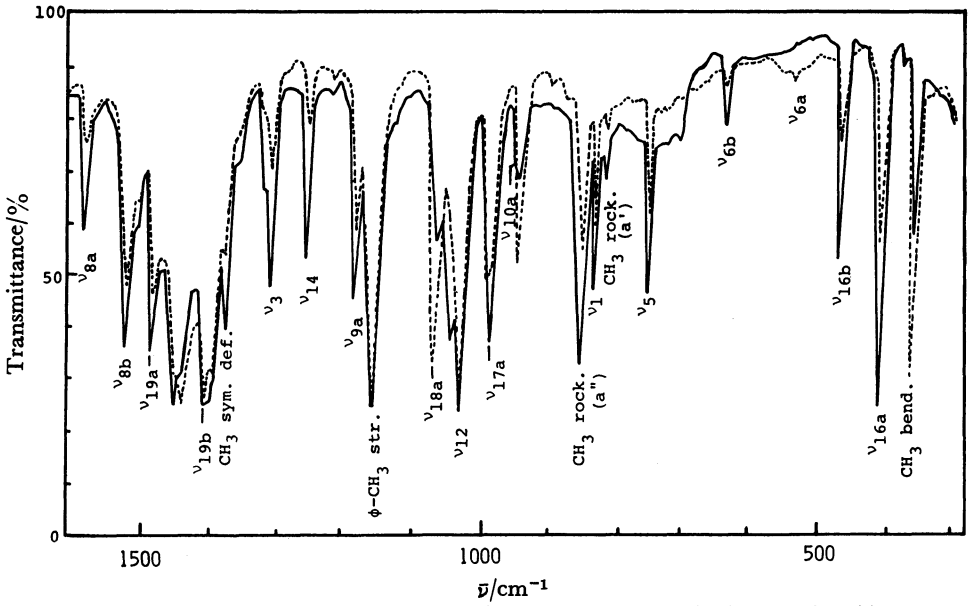


Fig. 2. Polarized infrared spectrum of 2-methylpyrazine single crystal at 77 K.

character. Normal coordinate and INDO calculations suggested that the transition moments of $CH_3$ bending, $\nu_{12}$ and $\nu_{18a}$ vibrations lie nearly along the molecular b axis, while those of $\nu_{6b}$, $\nu_{14}$, $\nu_3$, and $\nu_{19b}$ vibrations nearly along the molecular a axis. These results definitely indicate that the bands at 342, 1031, and 1065 cm$^{-1}$ should be assigned to $CH_3$ bending, $\nu_{12}$ and $\nu_{18a}$, respectively, and the bands at 631, 1255, 1308, and 1408 cm$^{-1}$ to $\nu_{6b}$, $\nu_{14}$, $\nu_3$, and $\nu_{19b}$ vibrations, respectively.

The in-plane vibrations, which correspond to the vibrations belonging to the $a_1$ and $b_2$ species in the point group $C_{2v}$, are the totally symmetric vibrations in 2-methylpyrazine. However, it is expected that the bands which come from the $a_1$ species will show strongly polarized character and the bands which come from the $b_2$ species will show somewhat depolarized character in the depolarization measurement of the Raman spectrum. Therefore, the strongly polarized Raman bands at 3056, 3038, 1580, 1480, 1176, 1058, 1022, 826, and 556 cm$^{-1}$ were assigned to $\nu_2$, $\nu_{13}$, $\nu_{8a}$, $\nu_{19a}$, $\nu_{9a}$, $\nu_{18a}$, $\nu_{12}$, $\nu_1$, and $\nu_{6a}$, respectively, and the depolarized Raman band at 1529 cm$^{-1}$ to $\nu_{8b}$. Polarized Raman bands at 1247, 1154, and 635 cm$^{-1}$ could be assigned to $\nu_{14}$, C–$CH_3$ stretching, and $\nu_{6b}$ vibrations, respectively, since calculation suggested that these vibrations have the transition moments nearly along the C–$CH_3$ bond.

*Out-of-plane Vibration*: Infrared bands observed at 404, 462, 751, and 831 cm$^{-1}$ in the vapor showed quite clearly a C band envelope and the corresponding infrared single crystal bands showed type A polarization character. Hence, these bands were assigned to the out-of-plane $\nu_{16a}$, $\nu_{16b}$, $\nu_5$, and $CH_3$ rocking vibrations (a″ species), respectively. The corresponding infrared single crystal bands showed type A polarization character. The other five out-of-plane vibrations of $\nu_{17a}$, $\nu_{10a}$, $\nu_4$, $CH_3$ wagging, and C–$CH_3$ torsional vibrations were assigned to depolarized Raman bands observed at 975, 929, 720, 203, and 169 cm$^{-1}$, respectively. The corresponding infrared single crystal bands at 985 and 948 cm$^{-1}$ showed type A character.

The characteristic vibrations for the $CH_3$ group were determined based on the observed polarization characters as well as on the normal coordinate calculation. The normal vibrations assigned are summarized in Table 3. The agreement between observed and calculated frequencies is satisfactory.

*Phosphorescence. Magnetic Effect on the Phosphorescence Lifetime*: Analysis of the phosphorescence decay observed at 1.4 K gave lifetimes of 6.2 and 80 ms in methylcyclohexane and 14 and 37 ms in *p*-dibromobenzene. We tried to identify the three sublevel decays through the MIDP technique, but the MIDP signals were too weak to detect the decays clearly. Therefore, the magnetic effect on the phosphorescence lifetime was studied in the *p*-dibromobenzene host single crystal at 1.4 K in order to investigate the emitting sublevels and to find the unknown third lifetime phosphorescence.

It is necessary to know what orientation a 2-methylpyrazine molecule takes in the *p*-dibromobenzene host crystal. The *p*-dibromobenzene single crystal is known to belong to the space group $P2_{1/a}$ with $Z=2$ and the

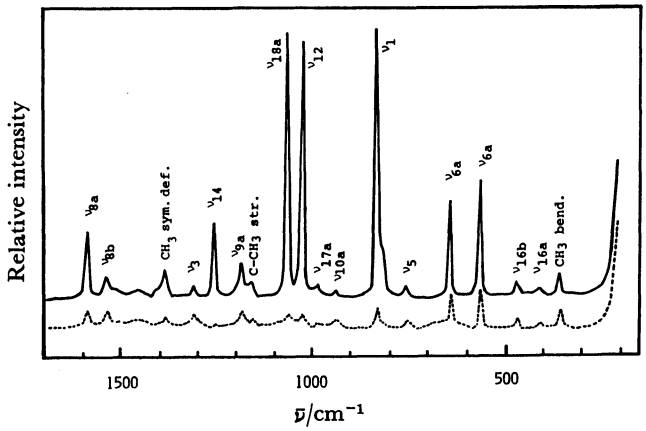


Fig. 3. Raman spectrum at room temperature.

TABLE 3. NORMAL VIBRATIONS OF 2-METHYLPYRAZINE

| Sym. species | Vibrational mode | Raman Liquid $\bar{\nu}$/cm$^{-1}$ | Rel. int. | Pol. | Infrared Single crystal $\bar{\nu}$/cm$^{-1}$ | Rel. int. | Pol. | Vapor Pol. | Calcd $\bar{\nu}$/cm$^{-1}$ |
|---|---|---|---|---|---|---|---|---|---|
| a′ | $\nu_2$ C–H str. | 3056 | 0.5 | p | | | | | 3058 |
| | $\nu_{13}$ C–H str. | 3038 | 1 | p | | | | | 3034 |
| | $\nu_{8a}$ Ring | 1580 | 2 | p | 1587 | 4 | A | | 1573 |
| | $\nu_{19a}$ Ring | 1480 | 0.1 | p | 1487 | 5 | A | A | 1489 |
| | $\nu_{9a}$ H bend. | 1176 | 1 | p | 1183 | 6 | A | | 1170 |
| | $\nu_{18a}$ H bend. | 1058 | 10 | p | 1063 | 7 | B | B | 1070 |
| | $\nu_{12}$ Ring | 1022 | 8 | p | 1027 | 9 | B | B | 1022 |
| | $\nu_1$ Ring | 826 | 10 | p | 830 | 5 | A | | 820 |
| | $\nu_{6a}$ Ring | 556 | 4 | p | 557 | 1 | B | | 552 |
| | $\nu_{7b}$ C–H str. | 3005 | 0.1 | ? | 3003[a] | 3 | | | 3004 |
| | $\nu_{8b}$ Ring | 1529 | 0.5 | dp | 1530 | 7 | A | | 1518 |
| | $\nu_{19b}$ Ring | 1395 | 0.3 | dp | 1405 | 9 | A | A | 1397 |
| | $\nu_3$ H bend. | 1300 | 0.5 | dp | 1309 | 6 | A | A | 1303 |
| | $\nu_{14}$ Ring | 1247 | 3 | p | 1254 | 5 | A | A | 1249 |
| | $\nu_{20b}$ C–$CH_3$ str. | 1154 | 0.5 | p | 1156 | 9 | A? | | 1154 |
| | $\nu_{6b}$ Ring | 635 | 4 | p | 640 | 2 | A | A | 637 |
| | $\nu_{15}$ $CH_3$ bend. | 352 | 1 | dp | 359 | 9 | B | B | 356 |
| a″ | $\nu_{17a}$ H wag. | 975 | 0.5 | dp | 985 | 6 | A | | 977 |
| | $\nu_{10a}$ H wag. | 929 | 0.5 | dp | 948 | 2 | A | | 925 |
| | $\nu_{16a}$ Ring | 405 | 0.3 | dp | 409 | 10 | A | C | 407 |
| | $\nu_5$ H wag. | 748 | 0.5 | dp | 752 | 6 | A | C | 750 |
| | $\nu_4$ Ring | 720 | 0.1 | ? | | | | | 718 |
| | $\nu_{16b}$ Ring | 464 | 0.5 | dp | 467 | 6 | A | C | 461 |
| | $\nu_{11}$ $CH_3$ wag. | 203 | 4 | dp | | | | | 202 |
| | C–$CH_3$ tor. | 169 | 0.2 | ? | | | | | 169 |
| Characteristic vibrations of $CH_3$ group | | | | | | | | | |
| a′ | Sym. C–H str. | 2928 | 2 | p | 2930[a] | 2 | | | 2931 |
| a′ | Antisym. C–H str. | 2865 | 0.2 | ? | 2867[a] | 0.5 | | | 2860 |
| a′ | $CH_3$ sym. def. | 1377 | 1 | p | 1376 | 4 | A | | 1377 |
| a′ | $CH_3$ degen. def. | 1440 | 0.1 | dp | 1438 | 6 | B | | 1441 |
| a″ | $CH_3$ degen. def. | 1450 | 0.2 | dp | 1448 | 6 | A | | 1456 |
| a′ | $CH_3$ rock. | 813 | 1 | dp | 816 | 2 | A | | 814 |
| a″ | $CH_3$ rock. | 840[b] | 0.2 | | 847 | 7 | A | C | 838 |

a) Vapor. b) Solid.

site group $C_i$. The van der Waals radii of the methyl group and of hydrogen and bromine atoms may suggest that a *p*-dibromobenzene molecule in the crystal is replaced by a 2-methylpyrazine molecule with the C–$CH_3$ bond parallel to the Br–Br direction. Thus, the 2-methylpyrazine molecule could take four different orientations; two of these are the same due to the $C_i$ site group symmetry. Therefore, the 2-methylpyrazine molecule could take two different orientations in the *p*-dibromobenzene crystal.

If the 2-methylpyrazine molecule could take two orientations equally, the intensity ratio of the 0-0 bands of the phosphorescences polarized along the b and a crystal axes would be calculated to be 1.9 from the crystal data given by Bezzi and Croatto.[15] The observed ratio was greater than 4 and no splitting of the 0-0 band of the unpolarized phosphorescence spectrum was observed under high resolution. These facts prove that the 2-methylpyrazine molecule could take only one orientation in the *p*-dibromobenzene host crystal.

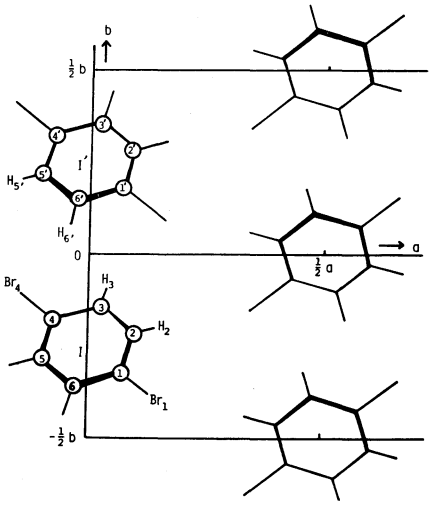


Fig. 4. Projection of *p*-dibromobenzene single crystal on the ab crystal plane.

The two nearest neighbor molecules, labeled I and I′, are shown in Fig. 4. The calculation of the intermolecular atomic distances using the crystal data showed that the distance of $H_3$–$H_{6'}$ is shorter than that of $H_3$–$H_{5'}$ and the distance of $H_3$–$C_{6'}$ is also shorter than that of $H_3$–$C_{5'}$. Thus, the hydrogen-hydrogen repulsion force between $H_3$ and $H_{6'}$ would be stronger than that between $H_3$ and $H_{5'}$ and the hydrogen bonding attraction between $H_3$ and $C_{6'}$ would be stronger than that between $H_3$ and $C_{5'}$, if $C_{6'}$ and $C_{5'}$ atoms are replaced with N atoms. These considerations clearly suggest that N atoms of 2-methylpyrazine should occupy the positions of $C_{3'}$ and $C_{6'}$, and thus, the N–N axis and the normal of the 2-methylpyrazine plane are nearly parallel to the b and c crystal axes, respectively.

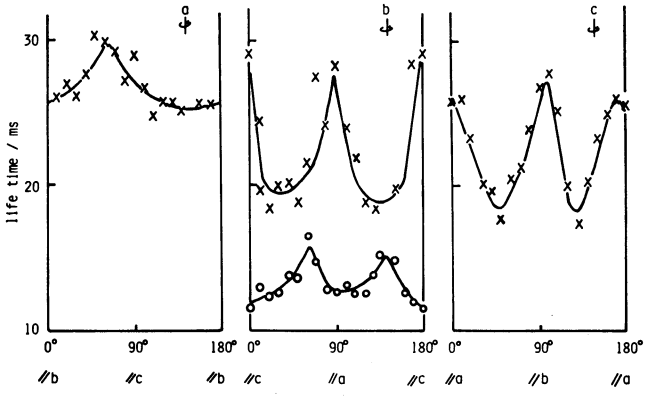


Fig. 5. Magnetic effect on the phosphorescence lifetime. a indicates rotation of the crystal about the a crystal axis. × and ○ indicate long and short lifetimes, respectively.

The magnetic effect on the phosphorescence lifetime is shown in Fig. 5. A remarkable change of the lifetime was observed for the long lifetime phosphorescence by rotation of the crystal about the a, b, and c crystal axes. If the third lifetime, which could not be resolved, were nearly equal to the short lifetime 14 ms, the observed long lifetime would become longer only when the spin axis of the long lifetime sublevel is parallel to the magnetic field. In other orientations of the spin axis, the long lifetime sublevel would mix with the short lifetime sublevels and the observed lifetime would become shorter. In other words, the observed long lifetime would become longer only at two orientations of the crystal, where the spin axis of the long lifetime sublevel is parallel to the magnetic field. But the observed results showed that the long lifetime became longer at more than two orientations of the crystal, as can be seen in Fig. 5. That is, the observed magnetic effect on the long lifetime phosphorescence did not support the assumption that the third lifetime is nearly equal to the short lifetime.

If the third lifetime is nearly equal to the long lifetime, 37 ms, the observed long lifetime would become longer whenever the spin axis of one of the two long lifetime sublevels is parallel to the magnetic field or whenever the spin axes of both the long lifetime sublevels are perpendicular to the magnetic field. In other words, a longer lifetime will be observed when any one of the three spin axes is parallel to the magnetic field. This is exactly consistent with the observation. Thus, it was concluded that the phosphorescence consists of three emission components: one is short and the others are long in lifetime, as in the cases of pyrazine[16] and 2,6-dimethylpyrazine.[17]

The magnetic effect on the short lifetime phosphorescence will be discussed next. An appreciable change of the lifetime was observed only for the rotation of the crystal sample about the b axis. This may suggest that the short lifetime sublevel would not be so sensitive to the mixing, compared with the long lifetime sublevel. Let the decay rate constants of the short and long lifetime sublevels be $k_s$ and $k_l$, respectively. If the two sublevels mix with each other with a mixing ratio of $a/b$, the rate constants $k_s$ and $k_l$ may change to $k_{s'}=ak_s+bk_l$ and $k_{l'}=ak_l+bk_s$, respectively, where $a+b=1$. Thus, the new short and long lifetimes are given by $\tau_{s'}=1/(ak_s+bk_l)$ and $\tau_{l'}=1/(ak_l+bk_s)$, respectively. The observed ratio of the rate constants $k_s/k_l$ was approximately 3/1. In our experiment, the magnetic perturbation was not strong enough and thus $a$ would be greater than $b$. Hence, the magnetic dependence on the short lifetime phosphorescence is expected to be much less sensitive than that on the long lifetime phosphorescence.

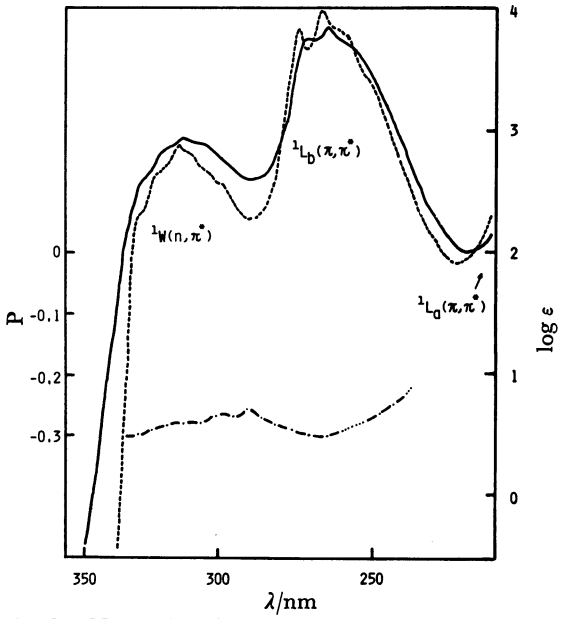


Fig. 6. Near ultraviolet absorption spectrum (—— at 20 °C, ------ at 77 K) and excitation polarization spectrum (-·-·-) monitoring the intensity of the 0-0 band of the phosphorescence at 77 K in EPA.

*Phosphorescence Process*: The excitation polarization spectrum obtained by the photoselection experiment in EPA at 77 K is shown in Fig. 6, together with the absorption spectrum. These spectra clearly indicate that the lowest triplet state is a $^3W(n, \pi^*)$ perturbed by the $^1L_a(\pi, \pi^*)$ state, as in the case of pyrazine. The coordinate axis for this molecule was taken in such a

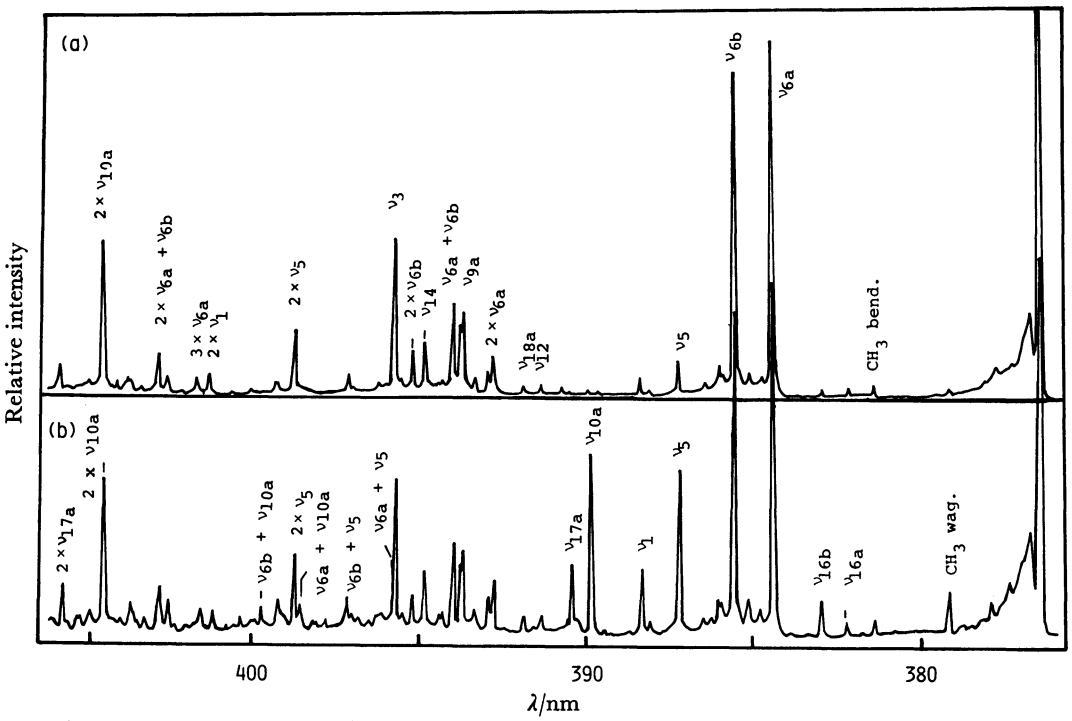


Fig. 7. Short (a) and long (b) lifetime phosphorescence spectra in methylcyclohexane at 1.4 K.

way that the x axis is perpendicular to the molecular plane and the z axis is along the N–N direction. Althrough the axis of the diagonalized spin functions of this molecule is not known, we could suppose that the x″ spin axis may coincide with the x axis and y″ and z″ spin axes would be roughly parallel to the y and x axes, respectively. The spin-orbit coupling matrix element between the $^1L_a(\pi, \pi^*)$ and $^3W(n, \pi^*)$ states gives the atomic integral of $\langle p_z|Hso|p_x\rangle$, where the most effective angular momentum operator is $L_y$. Hence, we may conclude that the short lifetime phosphorescence may arise from the y″ sublevel of the lowest triplet state, as in the case of pyrazine.

The time-resolved phosphorescence spectrum in methylcyclohexane at 1.4 K is shown in Fig. 7. The short lifetime phosphorescence spectrum was observed in the following way. The sample was excited for 5 ms and the excitation was cut off. 1 ms after ceasing the excitation, the phosphorescence was sampled for 5 ms. The observed spectrum might contain the bands due to the long lifetime phosphorescence, but their intensity is expected to be very weak; hence, all bands of the spectrum except for extremely weak bands could be safely ascribed to the short lifetime phosphorescence. The long lifetime phosphorescence was observed with 100, 100, and 100 ms of the excitation, waiting, and sampling times, respectively. Intensity ratio of the 0-0 bands of the long and short lifetime phosphorescence spectra at $t=0$, when the excitation of the sample was cut off, was calculated to be about 1/30. The spectra shown in Fig. 7 are drawn after normalizing the observed intensities of the 0-0 bands of the short and long lifetime phosphorescences to unity.

The vibrational analysis of the short lifetime phosphorescence will be discussed first. The shortest wavelength band at 376.55 nm, whose intensity is the strongest in the spectrum, was taken as the 0-0 band. Strong bands separated by 557, 636, 1175, 1248, and 1303 $cm^{-1}$ from the 0-0 band were assigned to $\nu_{6a}$, $\nu_{6a}$, $\nu_{9b}$, $\nu_{14}$, and $\nu_3$ vibrations, respectively. The overtone and combination bands of these vibrations were observed with medium intensity.

Medium intense bands separated by 750 and 926 $cm^{-1}$ from the 0-0 band were ascribed to $\nu_5$ and $\nu_{10a}$ vibrations, respectively. Progressions of the $\nu_5$ and $\nu_{10a}$ vibrations extending up to four quanta were observed with strong intensity in the even quanta and weak intensity in the odd quanta. Extremely weak bands assigned to $CH_3$ wagging, $\nu_{16a}$, $\nu_{16b}$, and $\nu_{17a}$ vibrations were also observed.

Although the long lifetime phosphrescence gave essentially the same spectral structure as that of the short lifetime phosphorescence, the most characteristic feature of the long lifetime spectrum was the remarkable intensification of the bands assigned to the out-of-plane $CH_3$ wagging, $\nu_{16b}$, $\nu_5$, $\nu_{10a}$, $\nu_{17a}$, and the totally symmetric $\nu_1$ vibrations. The bands assigned to the totally symmetric $\nu_{6a}$, $\nu_{6b}$, $\nu_{9a}$, $\nu_{14}$, and $\nu_3$ vibrations were also observed with strong intensity in the long lifetime spectrum.

The short lifetime phosphorescence cannot sneak into the long lifetime spectrum, because the population of the y″ sublevel must decay out during 100 ms of the waiting time for sampling the phosphorescence. Therefore, the bands assigned to the totally symmetric vibrations observed in the long lifetime spectrum should be ascribed to the bands arising from the x and/or z″ sublevels.

The time-resolved phosphorescence spectrum was also studied in *p*-dibromobenzene at 1.4 K. The short and

long lifetime phosphorescence showed essentially the same spectral structures as those observed in methylcyclohexane. The polarized long lifetime phosphorescence spectrum of 2-methylpyrazine doped in a *p*-dibromobenzene host single crystal was observed at 1.4 K. The phosphorescence spectra polarized along the a, b, and c crystal axes are shown in Fig. 8, where the intensity of the band polarized along the c axis was normalized to unity.

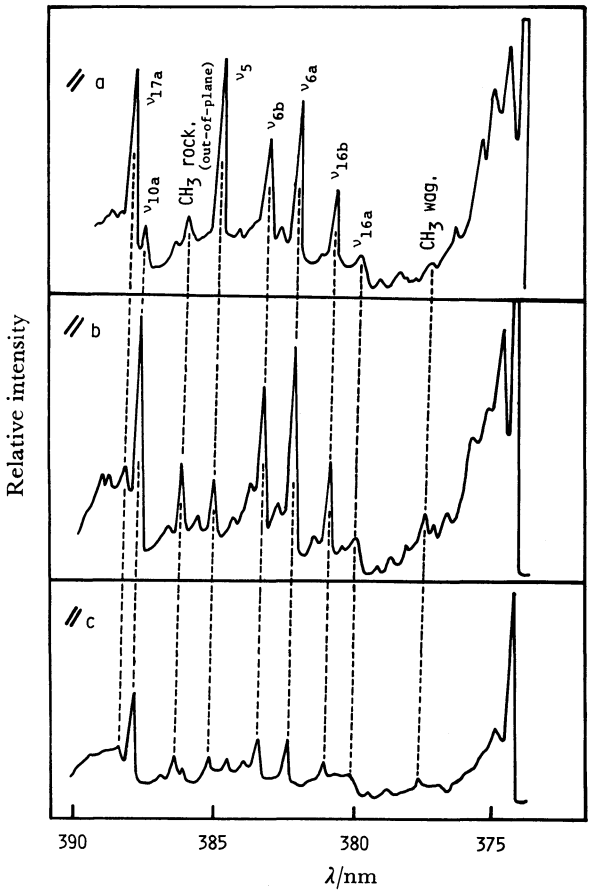


Fig. 8. Polarized long lifetime phosphorescence spectrum in *p*-dibromobenzene single crystal at 1.4 K.

Let the direction of the transition moments of the $^1W(n, \pi^*)\leftarrow S_0$, $^1L_b(\pi, \pi^*)\leftarrow S_0$, and $^1L_a(\pi, \pi^*)\leftarrow S_0$ absorptions be x, y′, and z′, respectively. The INDO calculation indicates that the z′ axis is in between the N–N and C–$CH_3$ axes and that the y′ axis is perpendicular to both x and z′ axes. Thus, we could suppose that the x, y′, and z′ axes are roughly parallel to the c, a, and b crystal axes, respectively.

Observed polarized spectra showed that the $\nu_5$ and $\nu_{17a}$ bands were strongly polarized along the a crystal axis, the bands ascribed to $CH_3$ wagging, $\nu_1$ and $\nu_{10a}$ vibrations were strongly polarized along the b axis, and the 0-0, $\nu_{6a}$, $\nu_{6b}$, $\nu_{16a}$, and $\nu_{16b}$ bands were equally polarized along the b and a axes. These observations indicate that the first two y′ polarized vibronic bands get their intensities from the $^1L_b\leftarrow S_0$, the second three z′ polarized bands from the $^1L_a\leftarrow S_0$, and the last five y′ and z′ polarized bands from the $^1L_a\leftarrow S_0$ as well as the $^1L_b\leftarrow S_0$ transitions.

TABLE 4. POLARIZATION DIRECTION OF THE PHOSPHORESCENCE BAND EMITTED FROM EACH SUBLEVELS OF THE LOWEST TRIPLET STATE

| Band | Sublevel | Polarization direction |
|---|---|---|
| 0-0 and in-plane vibronic | x | x |
| | y″ | y′, z′ |
| | z″ | y′, z′ |
| Out-of-plane vibronic | x | y′, z′ |
| | y″ | x |
| | z″ | x |

Polarization directions of the phosphorescence bands emitted from each sublevel of the lowest triplet state are given in Table 4. It was already concluded that the long lifetime phosphorescence consists of two emissions arising from x and z″ sublevels whose lifetimes are roughly equal. Table 4 definitely indicates that the y′ and z′ polarized 0-0 and totally symmetric vibronic bands should be attributed to the emission arising from the z″ sublevel, and the y′ and/or z′ polarized out-of-plane vibronic bands to the emission arising from the x sublevel.

The observed long progressions of the $\nu_5$ and $\nu_{10a}$ vibrations extending up to four quanta with strong intensity in the even quanta and relatively weak intensity in the odd quanta suggest that the potential surfaces for these normal coordinates would not be harmonic in the lowest triplet state. Such remarkable $\nu_5$ and $\nu_{10a}$ progressions are not observed in pyrazine, and thus the unharmonicity of the potentials for 2-methylpyrazine is expected to be much greater than that for pyrazine.

It should be noted that the observed long lifetime of about 80 ms for 2-methylpyrazine is much shorter than the longest lifetime of about 300 ms for pyrazine. This may be due to the low symmetry of the 2-methylpyrazine molecule caused by methyl substitution.

The authors wish to express their thanks to Dr. Motohiko Koyanagi for his valuable discussions. They are also indebted to Mr. Yoshinori Nibu for his help in the experimental work.

## References

1) L. Goodman and M. Kasha, *J. Mol. Spectrosc.*, **2**, 58 (1958).
2) K. K. Innes and L. E. Gidding, *Discuss. Faraday Soc.*, **35**, 192 (1963).
3) E. F. Zalewski, D. S. McClure, and D. L. Narva, *J. Chem. Phys.*, **61**, 2964 (1974).
4) A. A. Gwaiz and M. A. El-Sayed, *Chem, Phys. Lett.*, **19**, 11 (1973).
5) K. Matsuzaki, M. Sasaki, and T. Azumi, *J. Chem. Phys.*, **65**, 3326 (1976).
6) K. Matsuzaki and T. Azumi, *J. Chem. Phys.*, **69**, 3907 (1978).
7) N. Nishi, M. Kinoshita, T. Nakashima, R. Shimada, and Y. Kanda, *Mol. Phys.*, **33**, 31 (1979).
8) S. L. Madej, G. D. Gillispie, and E. C. Lim, *Chem. Phys.*, **32**, 1 (1978).
9) S. Kizuki, Y. Ishibashi, H. Shimada, and R. Shimada,

*Mem. Fac. Sci. Kyushu Univ., Ser. C*, **13**, 7 (1981).
10) Y. Urabe, T. Watanabe, Y. Ishibashi, H. Shimada, and R. Shimada, *Mem. Fac. Sci. Kyushu Univ., Ser. C*, **13**, 1 (1981).
11) M. Scrocco, C. di Lauro, and S. Califano, *Spectrochim. Acta*, **21**, 571 (1965).
12) F. A. Keidel and S. H. Bauer, *J. Chem. Phys.*, **25**, 1218 (1965).
13) P. Cossee and J. H. Schachtschneider, *J. Chem. Phys.*, **44**, 97 (1966).
14) T. Ueda and T. Shimanouchi, *J. Mol. Spectrosc.*, **28**, 350 (1968).
15) S. Bezzi and V. Croatto, *Gazz. Chim. Ital.*, **72**, 318 (1942).
16) D. M. Burland and J. Schmidt, *Mol. Phys.*, **22**, 19 (1971).
17) K. Niimori, K. Fukuda, N. Nishi, and M. Kinoshita, Symposium on the Molecular Structure and Molecular Electronic Structure, Tokyo, October 1974, Abstr. No. 20A10.